Published in final edited form as:
Magn Reson Med. 2010 March ; 63(3): 765–771. doi:10.1002/mrm.22245.

ESTIMATION OF LABELING EFFICIENCY IN PSEUDO-CONTINUOUS ARTERIAL SPIN LABELING

Sina Aslan[1], **Feng Xu**[1], **Peiying L. Wang**[1], **Jinsoo Uh**[1], **Uma S. Yezhuvath**[1], **Matthias van Osch**[2], and **Hanzhang Lu**[1,*]

[1] Advanced Imaging Research Center, UT Southwestern Medical Center, Dallas, TX, United States [2] Department of Radiology, Leiden University Medical Center, Leiden, The Netherlands

Abstract

Pseudo-Continuous Arterial Spin Labeling (pCASL) MRI is a new ASL technique that has the potential of combining advantages of Continuous-ASL and Pulsed-ASL. However, unlike CASL, the labeling process of pCASL is not strictly an adiabatic inversion and the efficiency of labeling may be subject-specific. Here three experiments were performed to study the labeling efficiency in pCASL MRI. First, the optimal labeling position was determined empirically to be approximately 84 mm below Anterior-Commissure Posterior-Commissure line in order to achieve the highest sensitivity. Second, an experimental method was developed to utilize phase-contrast velocity MRI as a normalization factor and to estimate the labeling efficiency in vivo, which was founded to be 0.86±0.06 (n=10, mean±SD). Third, we compared the labeling efficiency of pCASL MRI under normocapnic and hypercapnic (inhalation of 5% CO2) conditions, and showed that a higher flow velocity in the feeding arteries resulted in a reduction in the labeling efficiency. In summary, our results suggest that labeling efficiency is a critical parameter in pCASL MRI not only in terms of achieving highest sensitivity but also in quantification of absolute CBF in ml/min/100g. We propose that the labeling efficiency should be estimated using phase-contrast velocity MRI on a subject-specific basis.

Keywords

ASL MRI; cerebral blood flow; pCASL; Labeling Efficiency; Perfusion; Hypercapnia

INTRODUCTION

Arterial Spin Labeling (ASL) MRI is a non-invasive technique that can measure Cerebral Blood Flow (CBF) (1). ASL MRI have two major categories, Continuous ASL (CASL) (2–6) and Pulsed ASL (PASL) (7–13). CASL technique utilizes continuous adiabatic inversion whereas PASL employs a single inversion pulse. In CASL, due to long steady state tagging, this technique often has high power disposition and sometimes requires a second RF coil for spin labeling (14,15). Therefore, it has not be widely used compared to PASL (6,16), which is simpler in implementation.

The recently developed Pseudo Continuous ASL (pCASL) MRI is an intermediate technique between CASL and PASL (17–20). This technique utilizes a series of discrete RF pulses to mimic the CASL method for spin labeling. One of the most critical parameters of the

*Corresponding Author: Hanzhang Lu, Ph.D., Advanced Imaging Research Center, UT Southwestern Medical Center, 5323 Harry Hines Blvd., Dallas, TX 75390, hanzhang.lu@utsouthwestern.edu, Tel: 214-645-2761, Fax: 214-645-2744.

pCASL method that could affect perfusion quantification and the quality of perfusion images is the labeling efficiency, α, defined as (arterial blood in the control scan – arterial blood in the label scan)/2. Unlike CASL, the labeling process of pCASL is not strictly an adiabatic inversion. Thus the labeling efficiency may be dependent on B0 inhomogeneity, B1 inhomogeneity and flow velocity. Several studies have used numerical simulations to investigate the efficiency under different labeling schemes and conditions (18–20). However, due to heterogeneities across subjects, arterial locations, and physiologic states, it is desirable to experimentally determine the labeling efficiency for each pCASL scan.

Here, we studied the effect of labeling efficiency in pCASL and proposed an experimental method to estimate the efficiency in vivo. Three sets of studies were performed. First, we empirically determined the optimal anatomic location to achieve the best labeling efficiency. The CBF map with the highest signal intensity was chosen as the best possible location. Second, we estimated the labeling efficiency at the optimal position by using phase-contrast (PC) velocity MRI as a normalization factor, thereby providing a method to determine α for each subject. Third, we demonstrated that labeling efficiency may change depending on physiological state. Carbon Dioxide (CO2) is a potent vasodilator and results in an increase in arterial flow velocity. We compared α during hypercapnia (inhalation of 5% CO2) to that during normocapnia (room-air breathing). Based on these data, we propose that the labeling efficiency should be estimated by using PC velocity MRI on a subject-specific basis.

MATERIALS AND METHODS

General

Experiments were performed on a 3T MR system (Philips Medical Systems, Best, the Netherlands) using body coil transmission and head coil reception. The protocol was approved by the Institutional Review Board of University of Texas Southwestern Medical Center at Dallas. A total of 25 subjects (14 male, 11 females, 21–45 years of age) were consented before participating in the study. A balanced pCASL sequence was used following previous studies by Wu et al. and Wong (18,19). Imaging parameters for all pCASL experiments were identical: single-shot gradient-echo EPI, field-of-view (FOV)=240×240, matrix=80×80, voxel size=3×3 mm, 27 slices acquired in ascending order, slice thickness=5 mm, no gap between slices, labeling duration=1650 ms, post spin labeling delay=1525 ms, TR=4020 ms, TE= 14ms, SENSE factor 2.5, time interval between consecutive slice acquisitions=35.5 ms, number of controls/labels= 30 pairs, RF duration=0.5 ms, pause between RF pulses = 0.5 ms, labeling pulse flip angle=18°, bandwidth=2.7 kHz, echo train length=35, and scan duration 4.5 min. In addition, a high resolution T1 weighted image was acquired with the following parameters: MPRAGE sequence, TR/TE=8.3ms/3.8ms, flip angle=12°, 160 sagittal slices, voxel size=1×1×1 mm^3, FOV=256×256×160 mm^3, and duration 4 min.

Study 1

The purpose of this study was to experimentally determine the optimal location of labeling plane to achieve the highest sensitivity. Seven subjects participated in this study. With the imaging slices positioned at the same location, the labeling plane was varied to be 49, 63, 74, 84, 94, 119, 149 mm distal to the anterior-commissure (AC) posterior-commissure (PC) line (bottom panel, Fig. 1).

PCASL data were motion corrected using SPM5 (Wellcome Department of Imaging Neuroscience, London, UK). An in-house MATLAB (Mathworks, Natick, MA) program was used to calculate the difference between averaged control and label images. Then, the difference image was corrected for imaging slice delay time to yield CBF-weight image,

which was normalized to the Brain template from Montreal Neurological Institute (MNI) using SPM5. The normalized CBF-weighted image was spatially averaged and compared across different labeling positions.

Study 2

The goal of this study was to estimate labeling efficiency of pCASL method utilizing PC velocity MRI as a normalization factor. PC velocity MRI uses bipolar gradients to modulate the phase of flowing spins and, under the assumption of minimal velocity variation across a voxel and negligible outflow effect, can provide an estimation of flow velocity (21). Ten subjects were scanned by placing the labeling slab at the optimal position determined in Study 1. In addition to the pCASL scan, a time-of-flight (TOF) angiogram and a PC velocity MRI were performed. The TOF angiogram was performed to visualize the internal carotid arteries (ICA) and vertebral arteries (VA), and to correctly position the PC velocity MRI slice (Fig. 2b). The imaging parameters were: TR/TE/flip angle=23ms/3.45ms/18°, FOV=160×70×160mm^3, voxel size 1.0×1.0×1.5mm^3, number of slices =47, one saturation slab of 60mm positioned above the imaging slab to suppress the venous vessels, duration 1 min 26 sec. The slice of the PC velocity MRI was oriented perpendicular to the ICA and VA (Fig. 2b) and the parameters were: single slice, voxel size=0.45×0.45 mm^2, FOV=230×230 mm^2, TR/TE=20/7 msec, flip angle=15°, slice thickness=5 mm, maximum velocity encoding=80 cm/s, and scan duration=30 sec.

PC velocity MRI provides a quantitative measurement of blood flow velocity, v, in ICA and VA. The blood velocity can be converted to flow rate by integrating over the cross-section of the vessels. The flow, F, is calculated by:

$$F = \int v dA \quad [1]$$

The unit of F is ml blood/second, i.e. blood influx per unit time. The PC velocity MRI was conducted at the level of cervical spine C2 above the bifurcation of carotid arteries. Anatomy literature established that there are no extracranial branches at this level (22). VA, on the other hand, may have small branches perfusing spinal cord, which may cause an over-estimation of brain blood flow. Such branches, however, are not visible in the TOF angiogram, suggesting that the effect, if any, is minimal. Thus the value of F indicates the sum of blood flow of the whole brain. We then divided F by the intracranial mass (calculated from T1W image and by assuming brain density of ρ =1.06 g/ml (23)) and obtained the normalization factor, $f_{PC,AVG}$, which is the whole brain averaged blood flow in units of ml blood/sec/g brain or ml blood/min/100g brain. On the other hand, pCASL can also give an estimation of blood flow using an equation from Alsop and Detre (7):

$$f_{pCASL}(x,y,z) = \frac{\lambda \cdot e^{\left(\frac{\delta}{T_{1a}}\right)}}{-2\alpha \cdot M_b^0 \cdot T_1 \cdot \left[e^{\left(\frac{\min(\delta - w_z),0}{T_1}\right)} - e^{\left(\frac{-w_z}{T_1}\right)\left(1-\frac{T_{1RF}}{T_1}\right)} \right]} \times \Delta M(x,y,z) \quad [2]$$

where $f_{pCASL}(x,y,z)$ is the blood flow value at voxel (x,y,z) obtained from pCASL in ml blood/min/100g brain; α is the labeling efficiency; λ is the blood-brain partition coefficient (0.98 ml/gram (23)); δ is the arterial transit time of blood from the tagging plane to the imaging slice (assumed to be 2 seconds (7)); w is the delay between the end of labeling and the start of acquisition (1.525 seconds); T_1 is the brain tissue T_1 (1.165 seconds (24)); T_{1a} is the T_1 of arterial blood (1.624 seconds (25)); T_{1RF} is the is the T_1 in the presence of off-resonance irradiation (0.75 seconds (26)); M_b^0 is the value of equilibrium magnetization of

brain tissue, which was obtained from manual ROI drawing of thalamus in the control image by $M_b^0 = M_{thal}/(1 - e^{-TR/T_{1,thal}})$ and assuming $T_{1,thal}$ = 0.986 seconds (24). We chose to draw the ROIs in the thalamus because it is gray matter and the structure thickness is sufficient for manual drawing (cortical gray matter can be very thin). Note also that both ΔM and M_b^0 contain T2* effect and they tend to cancel out after the division.

The whole brain averaged blood flow from pCASL is then given by:

$$f_{pCASL,AVG} = \frac{1}{\alpha} \sum_{x,y,z} \left\{ \frac{\lambda \cdot e^{(\frac{\delta}{T_{1a}})}}{-2 \cdot M_b^0 \cdot T_1 \cdot \left[e^{(\frac{\min(\delta - w_z),0}{T_1})} - e^{(\frac{-w_z}{T_1})(1 - \frac{T_{1RF}}{T_1})} \right]} \times \Delta M(x,y,z) \right\} / N_{WB} \quad [3]$$

where N_{WB} is the total number of pCASL voxels inside the intracranial space. We can then equate the blood flow measured from PC velocity MRI and pCASL MRI, i.e. $f_{PC,AVG} = f_{pCASL,AVG}$, and the only unknown in the equation is α which is estimated. Conceptually, this normalization method can be viewed as follows: Adding up all the pCASL signals within the brain gives the total amount of MRI signal in arbitrary unit (a.u.). On the other hand, the phase contrast scan gives the total amount of CBF in ml/min. These two are essentially equivalent. Thus, one can obtain the "conversion rate" that indicates each unit of MR signal is worth how much CBF. Once the labeling efficiency is known, the absolute CBF map can be calculated with Eq. [2].

For data processing of PC velocity MRI, a preliminary ROI was drawn on each of the four arteries (left and right ICA, left and right VA) based on the magnitude image (Fig. 2d). The operator was instructed to trace the boundary of the targeted vessel without including adjacent vessels. A signal intensity threshold (2 × noise level) was then applied to the magnitude image to remove any background voxels and to obtain the final vessel mask. The final mask was applied to the velocity map (i.e. the phase image of PC velocity MRI, Fig. 2e) and the total flow, F, inside the mask was calculated according to Eq. [1].

Regional CBF values for gray and white matters were quantified by manually placing ROIs in corresponding regions for each subject.

Study 3

In the third study, we investigated whether or not the labeling efficiency in pCASL is dependent on the subject's physiologic state. Hypercapnia was induced using 5% CO2 breathing and it is known to increase blood flow in the entire brain. Eight subjects wore nose clips and breathed via a mouth piece while they were scanned in a supine position. End Tidal CO2 (etCO2), breathing rate (BR), heart rate (HR) and arterial oxygenation saturation (spO2) (Capnogard, Model 1265, Novametrix Medical Systems, CT, and MEDRAD, Pittsburgh, PA) were also monitored and recorded continuously on a laptop. The subjects first inhaled normal room-air for 7 minutes while TOF angiogram, pCASL, arterial PC velocity MRI, and sagittal sinus PC velocity MRI scans were performed. Then, the valve was switched to hypercapnia gas mixture (5% CO2, 74% N2 and 21% O2) contained within a Douglas bag. Based on our experience, we allotted two minutes of waiting time to allow the physiology to stabilize at the hypercapnic state. Then, we finalized our study by performing a pCASL, arterial PC velocity MRI, and saggital sinus PC velocity MRI scans.

Hypercapnia-induced changes in CBF-weighted signals, i.e. $\Delta M = S_{control} - S_{label}$, were calculated using pCASL MRI. These results were compared to those obtained from arterial

PC velocity MRI and sagittal sinus PC velocity MRI. The labeling efficiencies of pCASL under normocapnic and hypercapnic states were also estimated using methods described in Study 2.

RESULTS

Study 1

Figure 1 shows the CBF-weighted signal intensity as a function of labeling position. The average CBF maps for each position are shown at the top of Fig. 1. Quantitative analysis revealed that the averaged signal intensity is highest when the label plane is positioned at 84mm below the AC-PC line. For individual subjects, the peak location was 78.1±3.8mm (mean±SD). CBF-weighted signal at 149mm was significantly lower than all other labeling positions ($p<0.001$ for pair-wise t tests) due to B1 power decay of the body transmission coil at distant location. When the labeling plane is very close to the brain (49mm below AC-PC), the CBF-weighted signal is also lower than the peak signal ($p<0.005$), possibly due to the variant vessel orientation in this region.

Study 2

Figure 2 illustrates the slice location of PC velocity MRI and representative PC velocity images. Using the PC velocity MRI and T1W MPRAGE data, whole brain blood flow (F), intracranial volume and unit mass blood flow ($f_{PC,AVG}$) were calculated to be 730.1±97.1 ml/min (n=10, mean±SD), 1508.5±188.2ml and 46.0±6.3 ml/min/100g, respectively. Considering that the data analysis of PC velocity MRI involves manual ROI drawing and this step may introduce rater-dependence in the quantification of F, we performed an inter-rater reliability test by having two researchers (SA and FX) each processing 50 vessels with a range of sizes. We observed a high inter-rater reliability ($r^2=0.99$, $p<0.001$). Using the PC velocity MRI results and Eq. [3], the labeling efficiency of pCASL was estimated to be 0.86±0.06 (n=10, mean±SD, range 0.79–0.98), in good agreement with simulation results reported by Wu et al. (19). After the labeling efficiency is determined, absolute CBF maps were computed using Eq. [2]. Whole brain averaged gray and white matter CBF were 55.0±8.4 ml/min/100g and 21.0±5.2 ml/min/100g, respectively, with a gray/white ratio of 2.7±0.5. Table 1 shows regional CBF values for gray and white matters. Parietal white matter had smaller ($p<0.03$) CBF compared to frontal and occipital white matters. No other regional differences were found for cortical gray matter or white matter. CBF values of deep gray matter were between white matter and cortical gray matter.

Study 3

Inhalation of 5% CO2 increased the Et-CO2 from 40.2±3.8 mmHg to 49.1±2.4 mmHg (n=8, mean±SD), but did not change arterial oxygenation or heart rate significantly. On average, PC velocity MRI in ICAs and VAs showed a whole brain CBF increase of 59.6±24.3% comparing hypercapnia to normocapnia. For confirmation, we also performed PC velocity MRI in sagittal sinus, which showed similar increases (62.2±29.7%) in global CBF. For pCASL, if we do not consider the possible changes in labeling efficiency between normocapnia and hypercapnia, and just use the CBF-weighted signal, $\Delta M=S_{control}-S_{label}$ (as used in most ASL fMRI or physiologic challenge studies), the increases in ΔM were 40.1±20.3%. This is considerably lower ($p=0.01$) than that using PC velocity MRI. We attribute this discrepancy to a reduction in labeling efficiency from normocapnia to hypercapnia, which were estimated to be 0.95±0.10 (n=8, mean±SD) and 0.84±0.09, respectively ($p=0.025$, paired t test), using the method described in Study 2. Figure 3 shows absolute CBF maps of normocapnia, hypercapnia and difference between hypercapnia and normocapnia, after accounting for the labeling efficiency in each physiologic condition.

We note that the estimated labeling efficiency during normocapnia appears to be higher than that in Study 2. Aside from a possible contribution of age differences between the two groups (35±10 yrs and 29±7 yrs for studies 2 and 3, respectively), another potential reason is that the subject tends to slightly hyperventilate when breathing through the mouth piece. As a result, the flow may be lower than the regular breathing conditions, and the labeling efficiency becomes higher. This is confirmed from the whole brain flow values (46.0±6.3 ml/min/100g and 42.8±8.2 ml/min/100g for studies 2 and 3, respectively).

Finally, we studied the correlation between the labeling efficiency and arterial flow velocity across subjects and physiologic states (total 26 measurements) (Fig. 4). A significant correlation was observed ($r=-0.46$, $p=0.02$), in general agreement with predictions from numerical simulations (dashed curve in Fig. 4).

DISCUSSION

In this study, we investigated several questions related to labeling efficiency in pCASL MRI. We performed pCASL labeling at different anatomic locations and determined that labeling at 84mm below the AC-PC line yielded the highest signal intensity, although the curve was relatively flat within the range of 74–94mm. Next, we proposed an experimental method to estimate the labeling efficiency for each subject based on whole brain CBF obtained from PC velocity MRI. Finally, we demonstrated that the labeling efficiency is not only subject-dependent but can also vary with physiologic conditions, because arterial flow velocity may be altered with vascular challenge or neural activation. Based on these findings, we recommend that the labeling efficiency in pCASL MRI should be estimated on a subject-specific and physiologic-condition-specific basis.

ASL MRI is a powerful technique and, in recent year, many interests have developed to apply this technique to the studies of neurological and psychiatric disorders, a niche field conventionally occupied by SPECT and PET imaging. Researchers especially clinical-oriented ones often seek a technique that is quantitative, easy to implement (e.g. no coil change, no contrast agent), short in duration (e.g. 5 min), and covers the whole brain, similar to T1, T2, FLAIR or DTI techniques. In this regard, a few traits of pCASL MRI such as high sensitivity, large brain coverage, and no need for special hardware (18,19,27) are particularly attractive. Compared to conventional ASL methods, pCASL MRI introduces minimal number of new caveats. One new issue that may be specific to pCASL is the uncertainty in labeling efficiency, because the labeling mechanism of pCASL is no longer based on adiabatic inversion and any variations in B0, B1, or flow velocity may have a significant impact on the efficiency. This is particularly relevant when one aims to conduct quantitative comparison of CBF between patient populations or in the same population before and after medication. Therefore, an experimental method to quantify the labeling efficiency in pCASL may provide an important piece of puzzle in preparing ASL MRI for large scale clinical research or routine clinical MRI scan.

Several previous studies have pointed out the importance of labeling efficiency in pCASL. Wong conducted numerical simulations and showed that the labeling efficiency is lower when the resonance frequency is shifted from the center frequency due to B0 inhomogeneity (18). Wu et al. and Dai et al. have reported pCASL labeling efficiency by using CASL as a reference (19,20). They conducted pCASL and conventional CASL MRI in the same participants and the differences in signal amplitude are attributed to differences in labeling efficiencies. By further assuming the CASL labeling efficiency from previous simulations by Maccotta et al. (28), the labeling efficiency in pCASL was estimated. One potential confounding factor is that the simulation results may not be applicable for the specific hardware and sequence parameters used in a given study. A second drawback is that it is not

practical to conduct pCASL and CASL comparison in every study, thus the labeling efficiency cannot be estimated on a subject-by-subject basis. On the other hand, the approach used in the present study is independent of previous simulations and can be easily applied without changing RF coil.

The method to estimate labeling efficiency proposed in this study is based on normalization of pCASL signal with PC velocity MRI. The scan time for PC velocity MRI is only 0.5 min. However, in order to position the PC velocity MRI slice, a TOF angiogram was acquired in our study, adding another 1.5 min to the session duration. Therefore additional 2–3 minutes of scan time is needed for our proposed technique. This is an approximately 40–50% increase compared to a conventional ASL scan of about 5 minutes. This may be particularly challenging for clinical scans where the total duration of the session is less than 20 minutes. In addition, extra data processing is needed compared to conventional ASL. The processing of the PC velocity data involves manual drawing of four ROIs covering left/right internal carotid and vertebral arteries, respectively. Our processing scripts are optimized and this typically takes less than 3 minutes. At present, we are doing the processing offline because we are not using velocity information for any real time adjustment of the protocol. However, in the future if we were to determine the labeling position for each subject in real time, the online processing would indeed be helpful. We would need to work with our vendor to incorporate the processing scripts in the user interface. However, in terms of the algorithm and procedure, they are quite straightforward and fast.

In the estimation of labeling efficiency from Eq. 3, the values of several variables were assumed from reports in literature. The actual values in a voxel may be slightly different from the assumed values. This will introduce error in the estimation. In particular, if there are regional differences in arterial transit time, tissue T1 or blood-brain partition coefficient, CBF in some brain regions will be over-estimated while other regions will be under-estimated. As a consequence, even though the whole brain averaged CBF is still correct, the regional values may contain errors. This issue is not specific to the efficiency estimation technique proposed in this study, but is related to ASL CBF measurement in general. If an accurate relative CBF map can be obtained with ASL, our method of quantification will also be accurate. A well-known approach to reduce arterial transit time sensitivity is to use longer delay times (7). However, overall SNR will be low at long delay times.

The PC velocity MRI protocol used in this study is very short in duration (0.5 min) and is not triggered by cardiac cycle. As a result, cardiac pulsation effect causes some ghostings in the phase-encoding direction (anterior-posterior direction). To assess the potential errors of cardiac pulsation, we compared the flux values obtained from non-gated PC and a 15-phase gated PC in additional subjects. The difference between the two techniques was found to be <3%, similar to the results from literature (29). Considering a 10 fold difference in scan duration, we have used the non-triggered version in this study. Another potential approach to estimate the labeling efficiency is to directly image the vessels immediately above the labeling location and to measure the magnitude and sign of the blood magnetization. For example, a signal of $-M_0$ would indicate a 100% labeling efficiency. While this approach is conceptually straightforward, there have not been reports for either CASL or pCASL estimations. Possible reasons include technical challenges in high-resolution imaging of blood vessels and the outflow effect of moving spins.

When using a fixed labeling location (84mm below AC-PC line), a range of labeling efficiencies were observed across subjects. This is partly explained by variations in arterial velocity (Fig. 4) due to normal variance in vessel anatomy. If one measures vessel velocity at a few locations and determines the best labeling location for each subject (e.g. find locations where velocity is approximately 10cm/s), a more homogeneous labeling efficiency

may be achieved. However, to achieve this, more PC velocity scans are needed and the operator also needs to conduct analysis on the fly. In addition, within a subject, the arterial flow velocity may change from one day to another and even within the same day, due to drug treatment, ventilation level or even consumption of caffeine products. Therefore, it is recommended that the labeling efficiency in pCASL MRI be estimated for each subject in the same scan session. Furthermore, other factors such as B0 and B1 inhomogeneity may cause the labeling efficiency to be different across subjects. This is especially relevant in view of our finding that the optimal labeling location appears to be in the neck regions where different subjects may have different amount of dental works. The dental works will not only cause a variation in labeling efficiency, but also result in a decrease in SNR of the pCASL signals. These factors need to be considered in certain clinical studies. For example, in studies comparing elderly subjects, it may be useful to choose a higher labeling location to avoid susceptibility effect of dental works.

The findings from the present study need to be interpreted in the context of its limitations. The PC velocity scan itself may contain noise due to cardiac pulsation and physiologic fluctuations, which will be propagated to the CBF map. Cardiac pulsation is particularly relevant in that flow velocity varies at different phases of the cardiac cycle and this would result in a phase-specific variation in labeling efficiency. Thus the efficiency reported in the present study can only be considered as an averaged value across all phases of the cycle, similar to the cases of CASL (30). In addition, accurate velocity mapping at the neck regions require the RF and gradient coils to sufficiently cover the area. This was possible with our particular experimental setup. However, if the coil coverage is not long, table movement may be needed. The pCASL technique itself has specific limitations. While the labeling pulses were designed to have lower power compared to conventional CASL, it is still greater than the PASL technique and sometimes poses limitations on labeling duration, number of slices and minimal TR. Also, the addition of extra scans to the protocol is certainly a pitfall compared to conventional ASL. The signal sensitivity to B0 and B1 inhomogeneity as well as to velocity adds further complexity to the technique.

CONCLUSION

Labeling efficiency is a critical parameter in pCASL MRI not only in terms of achieving highest sensitivity but also in quantification of absolute CBF in units of ml/min/100g. We proposed an in vivo experimental method to estimate labeling efficiency using phase contrast MRI as a normalization factor.

Acknowledgments

We are grateful to Dr. Wen-Ming Luh at National Institute of Mental Health for helpful discussions. This study was supported in part by the VA IDIQ contract number VA549-P-0027 awarded and administered by the Dallas, TX VA Medical Center. The content of this paper does not necessarily reflect the position or the policy of the U.S. government, and no official endorsement should be inferred.

Grant Sponsors: NIH R01 MH084021, NIH R21 NS054916, NIH R21 EB007821, NIH R21 AG034318, NIH R21 R01 AG033106, Texas Instruments Foundation, Department of Veterans Affairs VA549P0027

References

1. Detre JA, Leigh JS, Williams DS, Koretsky AP. Perfusion imaging. Magn Reson Med. 1992; 23:37–45. [PubMed: 1734182]
2. Williams DS, Detre JA, Leigh JS, Koretsky AP. Magnetic resonance imaging of perfusion using spin inversion of arterial water. Proc Natl Acad Sci U S A. 1992; 89:212–216. [PubMed: 1729691]

3. Wang J, Zhang Y, Wolf RL, Roc AC, Alsop DC, Detre JA. Amplitude-modulated continuous arterial spin-labeling 3.0-T perfusion MR imaging with a single coil: feasibility study. Radiology. 2005; 235:218–228. [PubMed: 15716390]
4. Trampel R, Jochimsen TH, Mildner T, Norris DG, Moller HE. Efficiency of flow-driven adiabatic spin inversion under realistic experimental conditions: a computer simulation. Magn Reson Med. 2004; 51:1187–1193. [PubMed: 15170839]
5. O'Gorman RL, Summers PE, Zelaya FO, Williams SC, Alsop DC, Lythgoe DJ. In vivo estimation of the flow-driven adiabatic inversion efficiency for continuous arterial spin labeling: a method using phase contrast magnetic resonance angiography. Magn Reson Med. 2006; 55:1291–1297. [PubMed: 16673361]
6. Wong EC, Buxton RB, Frank LR. A theoretical and experimental comparison of continuous and pulsed arterial spin labeling techniques for quantitative perfusion imaging. Magn Reson Med. 1998; 40:348–355. [PubMed: 9727936]
7. Alsop DC, Detre JA. Reduced transit-time sensitivity in noninvasive magnetic resonance imaging of human cerebral blood flow. J Cereb Blood Flow Metab. 1996; 16:1236–1249. [PubMed: 8898697]
8. Kim SG. Quantification of relative cerebral blood flow change by flow-sensitive alternating inversion recovery (FAIR) technique: application to functional mapping. Magn Reson Med. 1995; 34:293–301. [PubMed: 7500865]
9. Golay X, Stuber M, Pruessmann KP, Meier D, Boesiger P. Transfer insensitive labeling technique (TILT): application to multislice functional perfusion imaging. J Magn Reson Imaging. 1999; 9:454–461. [PubMed: 10194717]
10. Hendrikse J, Lu H, van der Grond J, Van Zijl PC, Golay X. Measurements of cerebral perfusion and arterial hemodynamics during visual stimulation using TURBO-TILT. Magn Reson Med. 2003; 50:429–433. [PubMed: 12876722]
11. Petersen ET, Lim T, Golay X. Model-free arterial spin labeling quantification approach for perfusion MRI. Magn Reson Med. 2006; 55:219–232. [PubMed: 16416430]
12. Kwong KK, Chesler DA, Weisskoff RM, Donahue KM, Davis TL, Ostergaard L, Campbell TA, Rosen BR. MR perfusion studies with T1-weighted echo planar imaging. Magn Reson Med. 1995; 34:878–887. [PubMed: 8598815]
13. Yang Y, Frank JA, Hou L, Ye FQ, McLaughlin AC, Duyn JH. Multislice imaging of quantitative cerebral perfusion with pulsed arterial spin labeling. Magn Reson Med. 1998; 39:825–832. [PubMed: 9581614]
14. Wolff SD, Balaban RS. Magnetization transfer contrast (MTC) and tissue water proton relaxation in vivo. Magn Reson Med. 1989; 10:135–144. [PubMed: 2547135]
15. Detre JA, Alsop DC. Perfusion magnetic resonance imaging with continuous arterial spin labeling: methods and clinical applications in the central nervous system. Eur J Radiol. 1999; 30:115–124. [PubMed: 10401592]
16. Gunther M, Oshio K, Feinberg DA. Single-shot 3D imaging techniques improve arterial spin labeling perfusion measurements. Magn Reson Med. 2005; 54:491–498. [PubMed: 16032686]
17. Garcia, DMdBC.; Alsop, DC. Pseudo-continuous flow driven adiabatic inversion for arterial spin lableing. Proceedings of the 13th Annual Meeting of ISMRM; Miami Beach, FL, USA. 2005. (Abstract 9)
18. Wong EC. Vessel-encoded arterial spin-labeling using pseudocontinuous tagging. Magn Reson Med. 2007; 58:1086–1091. [PubMed: 17969084]
19. Wu WC, Fernandez-Seara M, Detre JA, Wehrli FW, Wang J. A theoretical and experimental investigation of the tagging efficiency of pseudocontinuous arterial spin labeling. Magn Reson Med. 2007; 58:1020–1027. [PubMed: 17969096]
20. Dai W, Garcia D, de Bazelaire C, Alsop DC. Continuous flow-driven inversion for arterial spin labeling using pulsed radio frequency and gradient fields. Magn Reson Med. 2008; 60:1488–1497. [PubMed: 19025913]
21. Haacke, EMBR.; Thompson, MR.; Venkatesan, R. Magnetic Resonance Imaging: Physical Principles and Sequence Design. Wiley-Liss; 1999. p. 944
22. Gray H. Gray's Anatomy: Gramercy. 1988:1248.

23. Herscovitch P, Raichle ME. What is the correct value for the brain--blood partition coefficient for water? J Cereb Blood Flow Metab. 1985; 5:65–69. [PubMed: 3871783]
24. Lu H, Nagae-Poetscher LM, Golay X, Lin D, Pomper M, van Zijl PC. Routine clinical brain MRI sequences for use at 3.0 Tesla. J Magn Reson Imaging. 2005; 22:13–22. [PubMed: 15971174]
25. Lu H, Clingman C, Golay X, van Zijl PC. Determining the longitudinal relaxation time (T1) of blood at 3.0 Tesla. Magn Reson Med. 2004; 52:679–682. [PubMed: 15334591]
26. Oguz KK, Golay X, Pizzini FB, Freer CA, Winrow N, Ichord R, Casella JF, van Zijl PC, Melhem ER. Sickle cell disease: continuous arterial spin-labeling perfusion MR imaging in children. Radiology. 2003; 227:567–574. [PubMed: 12663827]
27. Fernandez-Seara MA, Edlow BL, Hoang A, Wang J, Feinberg DA, Detre JA. Minimizing acquisition time of arterial spin labeling at 3T. Magn Reson Med. 2008; 59:1467–1471. [PubMed: 18506806]
28. Maccotta L, Detre JA, Alsop DC. The efficiency of adiabatic inversion for perfusion imaging by arterial spin labeling. NMR Biomed. 1997; 10:216–221. [PubMed: 9430351]
29. Spilt A, Box FM, van der Geest RJ, Reiber JH, Kunz P, Kamper AM, Blauw GJ, van Buchem MA. Reproducibility of total cerebral blood flow measurements using phase contrast magnetic resonance imaging. J Magn Reson Imaging. 2002; 16:1–5. [PubMed: 12112496]
30. Werner R, Norris DG, Alfke K, Mehdorn HM, Jansen O. Improving the amplitude-modulated control experiment for multislice continuous arterial spin labeling. Magn Reson Med. 2005; 53:1096–1102. [PubMed: 15844087]

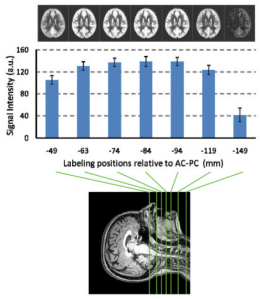

Fig. 1.

Intensity of CBF-weighted signal as a function of labeling position. PCASL MRI was performed with the labeling plane positioned at 7 different locations (bottom panel). The locations are in reference to the AC-PC line. The top panel shows average CBF-weighted images at each location. Image intensity change as a function of labeling position can be visually observed. Error bars indicate standard errors of mean.

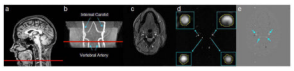

Fig. 2.

Phase-contrast (PC) velocity MRI of Internal Carotid Arteries (ICA) and Vertebral Arteries (VA). (a) Location of the slice of PC velocity MRI on a mid-sagittal image. (b) Location of the PC velocity MRI on the angiogram. (c) Raw image of PC velocity MRI. (d) Magnitude image of PC velocity MRI. The insets show the left and right ICAs and VAs as well as the manually drawn ROIs. (e) Velocity map from the PC velocity MRI. Positive value indicates inflow blood, often corresponding to arteries, whereas negative value indicates outflow blood, typically from veins.

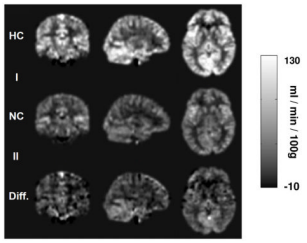

Fig. 3.

Representative CBF maps during normocapnia and hypercapnia as well their differences. The data have been spatially normalized to the MNI brain template. The quantification of CBF used Eq. [2] and the experimentally estimated labeling efficiency. CBF increases can be seen in the entire brain.

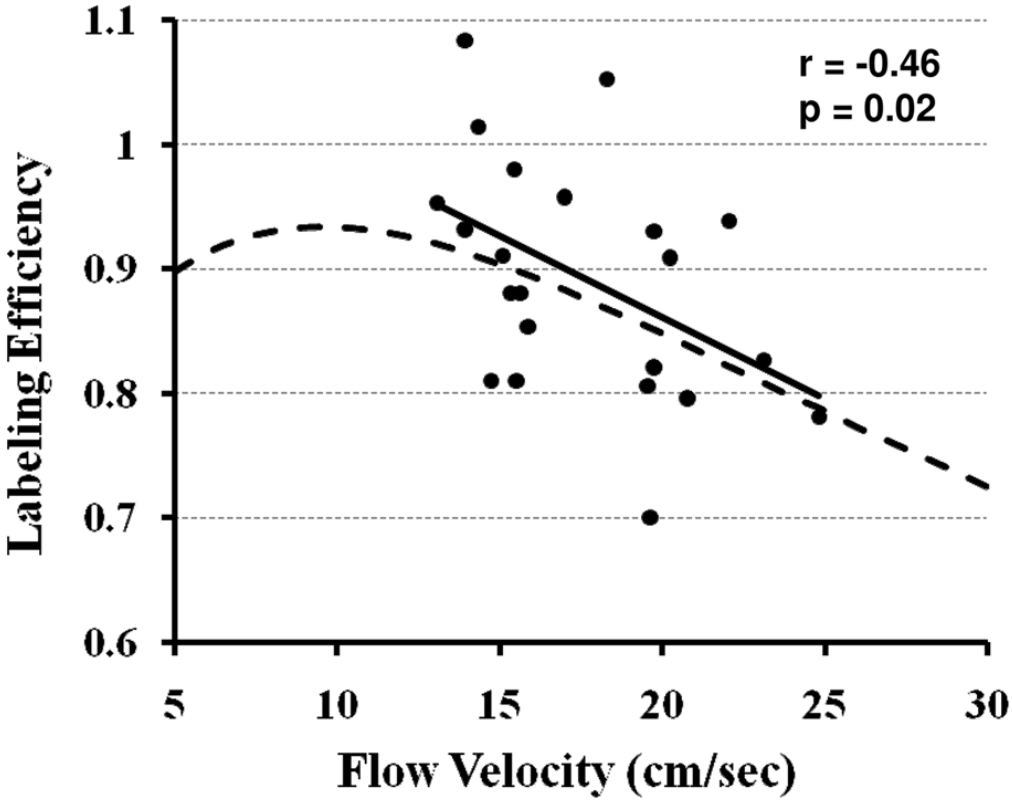

Fig. 4.

Experimental and simulation data of pCASL labeling efficiency as a function of flow velocity. The experimental data (filled dots) were from all subjects in Studies 2 and 3 (26 measurements). The solid line is the linear fitting of the experimental data. The simulation (dashed curve) used sequence parameters identical to those used in the experiments: RF duration=0.5 ms, pause between RF pulses=0.5 ms, labeling pulse flip angle=18°. The spins were assumed to be on-resonance and flowing at a constant velocity. The experimental data showed a significant correlation between labeling efficiency and flow velocity ($r=-0.46$, $p=0.02$).

Table 1

Regional CBF values (ml/min/100g) as measured from pCASL MRI (mean±SD, n=10).

Frontal gray matter	Parietal gray matter	Occipital gray matter	Frontal white matter	Parietal white matter	Occipital white matter	Caudate	Putamen
54.7±9.7	54.9±9.0	55.4±10.0	23.7±6.8	15.7±6.4	23.6±7.6	52.4±18.5	45.4±10.1